American Mineralogist, Volume 84, pages 1020–1026, 1999

Diogenites as asteroidal cumulates: Insights from spinel chemistry

LAURIE E. BOWMAN, JAMES. J. PAPIKE,* AND MICHAEL N. SPILDE

Institute of Meteoritics, Department of Earth and Planetary Sciences, University of New Mexico, Albuquerque, New Mexico 87131-1126, U.S.A.

ABSTRACT

The chemical composition of spinel was determined for a suite of 19 diogenites (orthopyroxenites) thought to be from asteroid 4 Vesta. Previous studies (Fowler et al. 1994, 1995) of orthopyroxene demonstrated that these diogenites are linked genetically, perhaps through fractional crystallization, in one or more crustal intrusions. The present study focuses on spinel to see if it also retains some chemical signatures of an igneous history. The chemical compositions across spinel grains reveal flat concentration profiles, indicating major subsolidus exchange with orthopyroxene. Nevertheless, significant chemical differences exist among the average spinel compositions from individual diogenites in the suite. A chemical continuum exists from high-Cr, low-Al spinel in diogenite LAP 91900 (Cr_20_3 60.7 wt%; Al_20_3 6.1 wt%) to low-Cr, high-Al spinel in diogenite ALHA 77256 (Cr_20_3 44.7 wt%; Al_20_3 21.8 wt%), which may represent one or more fractionation series. In these trends, Al and Ti behave as incompatible elements whose abundances increase with crystallization. These systematics differ from those in spinel in terrestrial or lunar basaltic systems because of the extremely Al-depleted nature of the diogenite parental melts. In terrestrial and lunar basalts, the increase in Al concentration in spinel is interrupted when plagioclase crystallizes. In diogenite parental melts, plagioclase does not come onto the liquidus until the very end of spinel crystallization.

INTRODUCTION

Magmatism on some asteroids involved extensive melting at ~4.6 Ga. Magmatic activity on one asteroid, possibly 4 Vesta (Consolmagno and Drake 1977; Drake 1979; Binzel and Xu 1993) gave rise to a series of related lithologies, which are designated howardites, eucrites, and diogenites or "HED." Eucrites are pigeonite-plagioclase basalts; diogenites are orthopyroxenites; and, as a first approximation, howardites are two-component brecciated mixtures of eucrites and diogenites. Eucrite, howardite, and diogenite members of the achondrite meteorites are considered to be related genetically (Mason 1967; Stolper 1977; Takeda et al. 1979; Bartels and Grove 1991; Grove and Bartels 1992). The relationship between eucrites and diogenites has been described in terms of fractional-crystallization and partial-melting models. In fractional-crystallization models (Mason 1967; Warren 1985; Warren and Jerde 1987; Bartels and Grove 1991; Grove and Bartels 1992), eucrites and diogenites represent a complementary continuum of fractional-crystallization products: diogenites corresponding to crystal accumulation during the crystallization of primary magmas at shallow to deep levels in the eucrite parent body (EPB) and eucrites being the residual melts. Alternatively, some experimental studies suggest that eucrites represent partial melts of a primitive, chondritic EPB mantle (Stolper 1977; Consolmagno and Drake 1977). Within this type of model, diogenites are still generally considered to be cumulates, but their petrogenetic relationship to the eucrites is not clear.

Recently, models similar to that of Mason (1967) involving large-scale melting and differentiation by magma-ocean processes have been proposed by Ruzicka et al. (1997), Takeda (1997), Righter and Drake (1997), and Warren (1997). A different and more complex model involving several batches of partial melts and fractional crystallization was proposed by Shearer et al. (1997). Most of our data for this model derive from major, minor, and trace element analyses of orthopyroxene (Fowler et al. 1994, 1995).

In this paper, we focus on the mineral spinel, which is a minor but important phase in diogenites. Bowman et al. (1997) found that spinel makes up ~0.9 vol% of a suite of diogenites. Chromite (Cr-spinel) is considered a valuable petrogenetic indicator. Chromites that formed in basalt in different geologic environments have distinct compositions. These differences are typically attributed to differences in the parental-melt compositions from which the spinel crystallized (Roeder and Reynolds 1991). As crystallization progresses, the melt composition changes and the chromite composition changes accordingly. For example, in terrestrial chromites, the most magnesian compositions are associated with forsteritic olivine in primitive basalts, mantle peridotites, and chromitites. Therefore, the most primitive chromite is expected to be that with the lowest Fe/(Fe+Mg). Additionally, the highest Cr/(Cr+Al+Ti) of chromite in basalt may reflect crystallization from a melt derived from a previously depleted source with Al removed (Roeder and Reynolds 1991). In terrestrial basalts, the earliest chromite to crystallize is higher in Mg and Cr, and lower in Ti and Al. Sack et al. (1991) and Mittlefehldt (1994) reported chemical data on diogenite spinel and demonstrated that Cr and Al are anticorrelated.

*E-mail: jpapike@unm.edu

0003-004X/99/0708–1020$05.00

The main objective of this paper is to determine whether or not spinel preserves a magmatic signature. A study by Berkley and Boynton (1992) suggested that diogenites originated from a series of magmas. If spinel does retain magmatic compositions, which have not been reset by metamorphism, then the spinel may reveal genetic linkages between magma bodies, linked perhaps by fractionation. Compositional trends in the diogenite chromites can be evaluated using a simple igneous fractionation model similar to that done by Fowler et al. (1994) for orthopyroxenes from this same suite of samples. A simple model for this petrogenesis would be the melting of a source previously depleted by removal of eucrite melt, and subsequent transport of this magma to the upper crust where orthopyroxene and spinel crystallized. Shearer et al. (1997) found that diogenites most likely represent fractional crystallization products of compositionally distinct batches of basaltic magma in shallow layered intrusions, as opposed to continuous fractional crystallization of a single magma. This paper attempts to find any relationships that can be interpreted by fractionation of either a single or multiple batches of magma.

TABLE 1. Diogenite-suite thin sections for chromite analyses

1	Aioun el Atrouss 12 UNM 1032
	Aioun el Atrouss 12 UNM 1034
	Aioun el Atrouss 12 UNM 1036
2	Ellemeet UNM 208
3	Garland 2140-6
4	Ibbenburen 3251
5	Johnstown 1031
	Johnstown 1033
6	Manegaon
7	Peckelsheim
8	Roda Me 1376
9	Shalka USNM 244-2
	Shalka Me 572
10	ALHA 77256, 115
	ALHA 77256, 116
11	EET 83246, 17
12	EET 83247, 13
13	EET 87530, 4
14	EETA 79002, 145
	EETA 79002, 155
15	LAP 91900, 19
16	LEW 88008, 12
17	LEW 88679, 5
18	PCA 91077, 7
19	TIL 82410, 16

ANALYTICAL TECHNIQUES

Twenty-nine thin sections representing 23 of the 24 known diogenites were available, but no analyzable chromites were found in four sections. Major and minor elements in chromite from the remaining 25 thin sections, representing 19 samples (Table 1), were analyzed using a JEOL 733 Superprobe equipped with an Oxford LINK eXL II operating system. All analyses were performed using an accelerating voltage of 15 kV and a beam current of 20 nA. The analytical setup was calibrated using natural mineral and metal standards with counting times of 20 s for major elements and 30 s for minor elements. ZAF corrections were applied to all analyses. Vanadium concentrations were corrected for interference from the Ti$K\alpha$ peak, resulting in a slight downward adjustment to the V concentration and totals (Snetsinger et al. 1968). All Fe in spinel is calculated as Fe^{2+} based on stoichiometric totals; Cr is assumed to be present as Cr^{3+} and V as V^{3+}. Individual microprobe analyses were rejected if the oxide total was not 100 ± 2 wt%, or if the sum of the cations (normalized to four O atoms) was not 3.00 ± 0.03 atoms per formula unit (apfu). Of the approximately 900 chromite analyses obtained, approximately 500 met the above criteria. Only acceptable analyses are plotted in the diagrams and used for the averages reported in Table 2. The lower level detection limits in weight percent of the oxides are as follows: SiO_2 = 0.04, Al_2O_3 = 0.16, TiO_2 = 0.06, Cr_2O_3 = 0.40, MgO = 0.11, FeO = 0.63, MnO = 0.10, CaO = 0.03, and NiO = 0.08. The lower detection limit of V_2O_3 is calculated at 0.16 wt% including error from the Ti interference correction.

RESULTS

Compositional zoning and grain traverses

Approximately 20 to 50 microprobe analyses per thin section were obtained on grains that were as large and unbrecciated as possible. However, the scarcity of chromite in most sections and the ubiquitous brecciation forced us in some cases to analyze grains of whatever shap and size were available. Analyses were performed on chromites within orthopyroxene grains, interstitial chromites between orthopyroxene grains, and chromites that had clearly reacted with or formed from reaction of the surrounding grains (Fig. 1, Bowman et al. 1997). Analyzed grain sizes ranged from ~10 mm to ~1 mm. The larger grains were analyzed using rim-to-rim traverses, consisting of multiple analytical points. Paired core and rim analyses or rim-core-rim analyses were taken on smaller grains, depending on their size.

Figure 1 shows traverses for the elements Fe, Mg, Cr, Al, and Ti on chromite grains in four representative samples: Aioun El Atrouss, ALHA 77256, EET 83247, and Johnstown. These examples include grain traverses for the different sizes and types of grains found in the entire suite of samples; a number of grains were traversed within each sample. Some of the smallest chromite grains analyzed were those in Manegaon, whereas ALHA 77256 contained some of the largest chromites analyzed. As is evident from these traverses, little zoning was found in any of the chromite grains, regardless of size or type. However, even though each grain has virtually constant composition, there is a notable range of Cr and Al concentrations among the analyzed grains. The other elements (Fe, Mg, and Ti) exhibit even less variability among individual grains. Therefore, based on the relatively homogenous composition of each grain, the grain traverses were averaged, and the sample averages are those of the grain averages (Table 2).

Cr, Al, and Ti systematics

The Cr, Al, and Ti ranges for each sample are plotted in Figure 2 in order of increasing Ti. Most samples show limited ranges of composition, although ranges of up to 0.5 apfu in a single diogenite are evident. Overall, Cr varies from a minimum of 1.00 apfu in EET 83246 to a maximum of 1.66–1.76 apfu in LAP 91900 (Fig. 2). Aluminum, on the other hand, is at a minimum in LAP 91900 at 0.2 apfu and a maximum of 1.0 apfu in EET 83246. Ellemeet and EET 83246 display the greatest range of both Cr and Al concentrations. The abundance of Ti is low in all samples, and ranges from nearly zero in Ellemeet to 0.045 apfu in Roda. Peckelsheim shows the greatest range in Ti

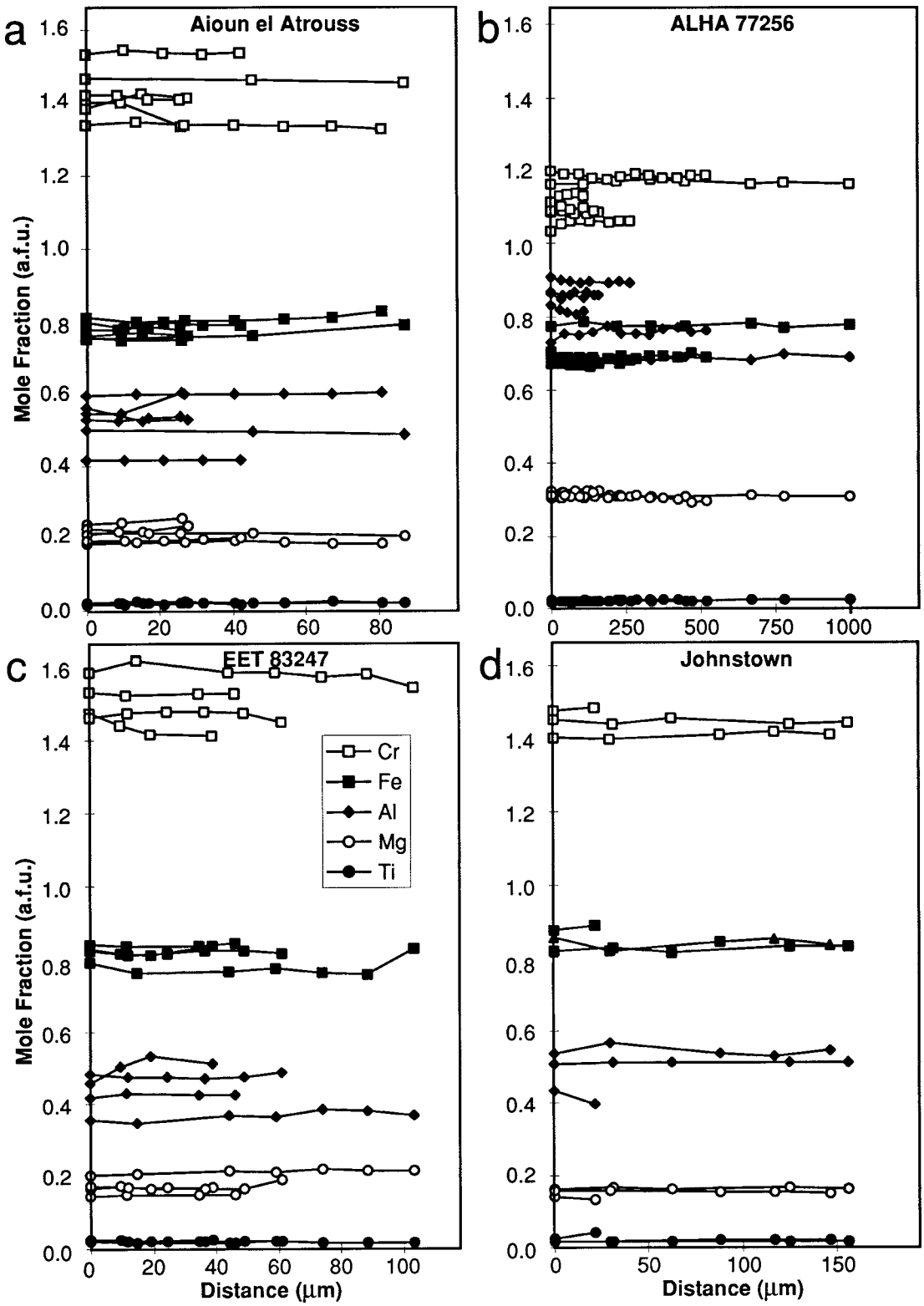

FIGURE 1. Microprobe traverses on individual spinel grains in selected diogenites: **(a)** Aioun El Atrouss; **(b)** ALHA 77256; **(c)** EET 83247; and **(d)** Johnstown. Most grains show little or no compositional zoning in major or minor elements. Distance in micrometers from edge to edge of each grain.

TABLE 2. Average diogenite chromite compositions

Sample	Aioun el Atrouss	Ellemeet	Garland	Ibbenburen	Johnstown	Manegaon	Peckelsheim	Roda	Shalka
No. of analyses	47	25	35	18	20	8	20	9	40
				Oxide wt%					
SiO_2	0.04	<0.04	<0.04	0.04	<0.04	0.22	<0.04	0.05	<0.04
Al_2O_3	13.20	15.63	7.27	9.85	11.98	13.41	10.43	12.43	7.25
TiO_2	0.79	0.11	0.39	0.82	0.62	0.62	0.85	1.47	0.48
Cr_2O_3	52.56	50.01	58.58	55.12	53.55	52.51	53.98	51.04	58.45
MgO	4.21	3.75	3.21	2.64	3.11	4.62	2.79	3.64	3.44
FeO	27.44	28.06	27.51	28.85	28.83	26.84	29.41	28.41	27.35
MnO	0.52	0.57	0.65	0.67	0.63	0.74	0.55	0.58	0.61
CaO	<0.03	<0.03	<0.03	0.11	<0.03	0.08	<0.03	0.12	<0.03
V_2O_3	0.45	0.78	0.83	0.54	0.35	0.48	0.65	0.35	0.97
NiO	<0.08	<0.08	<0.08	0.11	<0.08	0.11	<0.08	<0.08	<0.08
Total	99.17	98.91	98.44	98.75	99.07	99.63	98.66	98.09	98.55
				Formula proportions of cations based on four O atoms					
Si	<0.01	<0.01	<0.01	<0.01	<0.01	0.01	<0.01	<0.01	<0.01
Al	0.53	0.62	0.30	0.41	0.49	0.53	0.43	0.51	0.30
Ti	0.02	<0.01	0.01	0.02	0.02	0.02	0.02	0.04	0.01
Cr	1.41	1.34	1.64	1.53	1.46	1.40	1.49	1.40	1.63
Mg	0.21	0.19	0.17	0.14	0.16	0.23	0.15	0.19	0.18
Fe	0.78	0.79	0.81	0.85	0.83	0.76	0.86	0.82	0.81
Mn	0.02	0.02	0.02	0.02	0.02	0.02	0.02	0.02	0.02
Ca	<0.01	<0.01	<0.01	<0.01	<0.01	<0.01	<0.01	<0.01	<0.01
V	0.01	0.02	0.02	0.02	0.01	0.01	0.02	0.01	0.03
Ni	<0.01	<0.01	<0.01	<0.01	<0.01	<0.01	<0.01	<0.01	<0.01
Total	2.99	2.98	2.98	2.98	2.99	2.98	2.99	2.98	2.98

continued next page

(0.03 apfu) and has appreciable ranges in Al and Cr as well.

The abundances of Cr, Al, and Ti were evaluated for possible mutual correlations. As expected, Cr and Al are linked by simple substitution (Fig. 3), as revealed by a definite negative linear trend from LAP 91900 with high Cr and low Al, to ALHA 77256 with low Cr and high Al. Spinels from lunar mare basalts (data from Papike et al. 1976) are shown for comparison in Figure 3. The lunar spinels do not show a strong negative correlation between Cr and Al. Moreover, the lunar spinels do not achieve the high Al concentration found in diogenite spinels because the onset of plagioclase crystallization limited Al enrichment in the lunar case. Diogenite melts are initially de-

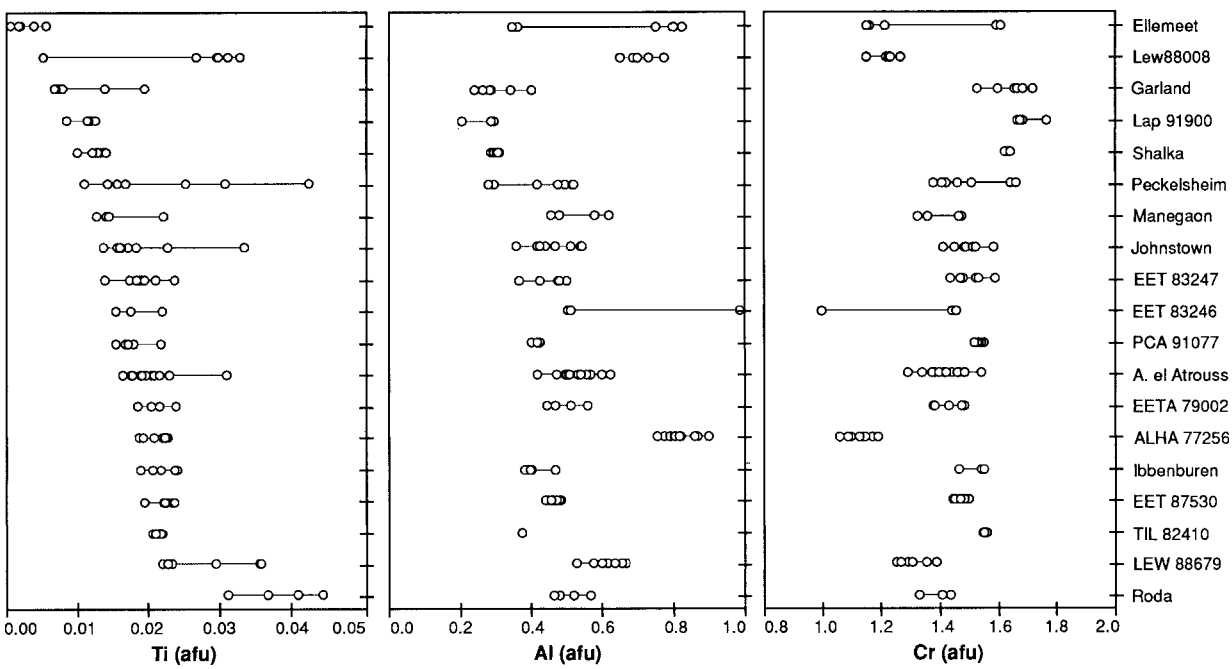

FIGURE 2. Average Ti, Al, and Cr concentrations for each spinel grain analyzed in each of the 19 samples, plotted in order of increasing Ti. Lines indicate the range of concentration in individual diogenites. Afpu = atoms per formula unit. Variations in Ellemeet, Peckelsheim, and ET 83246 may reflect multiple sources and the polymict nature of the breccias.

TABLE 2.—*Continued*

Sample	ALHA 77256	EET 83246	EET 83247	EET 87530	EETA 79002	LAP 91900	LEW 88008	LEW 88679	PCA 91077	TIL 82410
No. of analyses	77	16	29	62	13	17	39	26	14	33
					Oxide wt%					
SiO_2	<0.04	0.07	0.04	<0.04	0.07	<0.04	<0.04	0.25	<0.04	<0.04
Al_2O_3	21.81	17.10	11.07	11.40	12.56	6.11	17.85	15.22	10.06	9.09
TiO_2	0.88	0.72	0.73	0.86	0.82	0.42	1.02	1.07	0.67	0.81
Cr_2O_3	44.67	48.56	54.93	54.00	52.48	60.70	45.86	48.39	55.14	56.21
MgO	6.56	3.52	3.52	3.49	3.83	2.57	2.76	3.49	3.05	3.24
FeO	25.67	28.57	27.93	28.32	27.96	27.97	30.80	29.11	28.46	28.49
MnO	0.49	0.51	0.62	0.59	0.66	0.65	0.62	0.62	0.60	0.59
CaO	<0.03	<0.03	<0.03	<0.03	<0.03	<0.03	<0.03	0.12	<0.03	<0.03
V_2O_3	0.42	0.30	0.46	0.62	0.40	0.55	0.49	0.53	0.41	0.71
NiO	<0.08	<0.08	<0.08	<0.08	<0.08	<0.08	<0.08	0.09	<0.08	<0.08
Total	100.50	99.35	99.30	99.28	98.78	98.97	99.40	98.89	98.39	99.14
					Formula proportions of cations based on four O atoms					
Si	<0.01	<0.01	<0.01	<0.01	<0.01	<0.01	<0.01	0.03	<0.01	<0.01
Al	0.82	0.67	0.45	0.46	0.51	0.26	0.71	0.61	0.42	0.37
Ti	0.02	0.02	0.02	0.02	0.02	0.01	0.03	0.03	0.02	0.02
Cr	1.13	1.30	1.50	1.47	1.43	1.71	1.22	1.30	1.53	1.55
Mg	0.31	0.17	0.18	0.18	0.20	0.14	0.14	0.18	0.16	0.17
Fe	0.68	0.80	0.81	0.82	0.80	0.83	0.87	0.83	0.84	0.83
Mn	0.01	0.01	0.02	0.02	0.02	0.02	0.02	0.02	0.02	0.02
Ca	<0.01	<0.01	<0.01	<0.01	<0.01	<0.01	<0.01	0.01	<0.01	<0.01
V	0.01	0.01	0.01	0.02	0.01	0.02	0.01	0.01	0.01	0.02
Ni	<0.01	<0.01	<0.01	<0.01	<0.01	<0.01	<0.01	<0.01	<0.01	<0.01
Total	2.99	2.98	2.98	2.98	2.99	2.98	2.99	3.01	2.99	2.99

pleted in Al (Fowler et al. 1994, 1995). Modal analysis of twenty-three of the known diogenites indicates that plagioclase makes up only 0.4 vol% on average (Bowman et al. 1997). Thus, little plagioclase co-crystallized with spinel in diogenites, so that Al was incorporated perferentially into the spinel.

The plots of Ti show more scatter, but trends are observed here as well. The plot of Ti vs. Al (Fig. 4) shows a weak positive linear trend, which includes most of the diogenites, again from LAP 91900 with lower Ti and Al, to LEW 88008 and ALHA 77256, with higher Ti and Al. Ellemeet, which has a negligible Ti concentration, plots off the trend as an outlier. Roda is also an outlier, having the highest Ti value of 0.04 apfu.

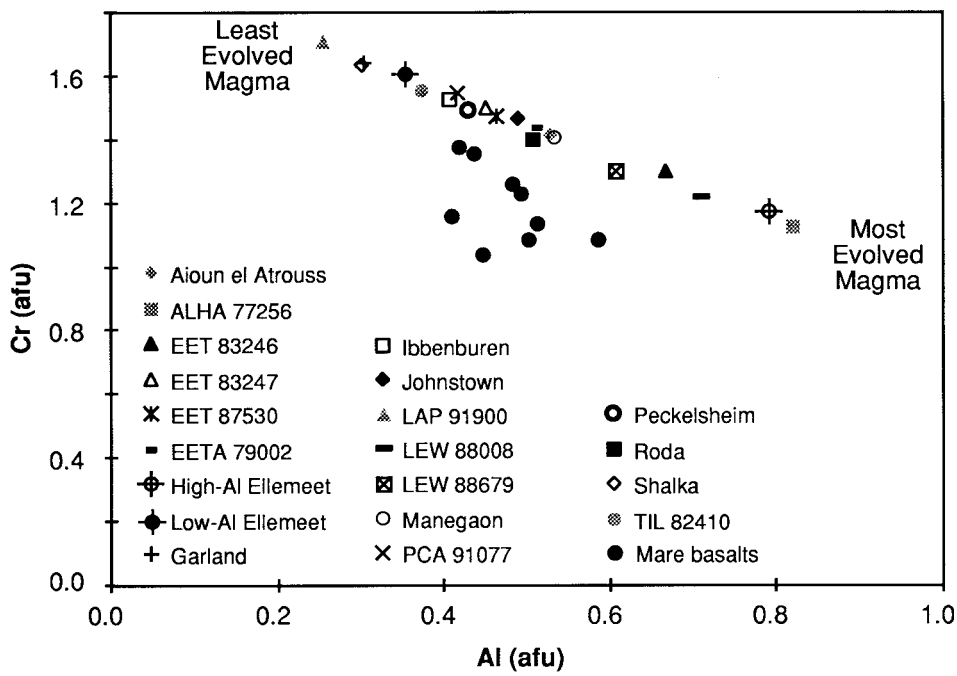

FIGURE 3. Average concentrations of Cr vs. Al for each sample. Data for selected mare basalts are plotted for comparison (from Papike et al. 1976). The magmatic crystallization trend is from least evolved magma with high Cr and low Al to more evolved magma with lower Cr and higher Al.

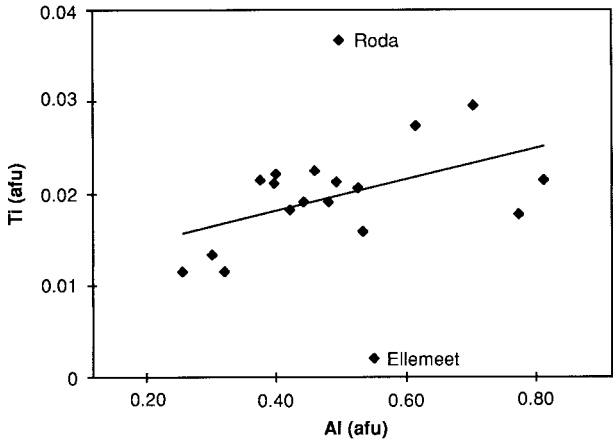

FIGURE 4. Average concentrations of Ti vs. Al for each diogenite. Samples show a magmatic trend of crystallization from the least evolved magma with low Ti and Al to crystallization from the most evolved magma with higher Ti and Al. Trend line is fitted by linear regression, excluding the outliers Roda and Ellemeet. Afpu = atoms per formula unit.

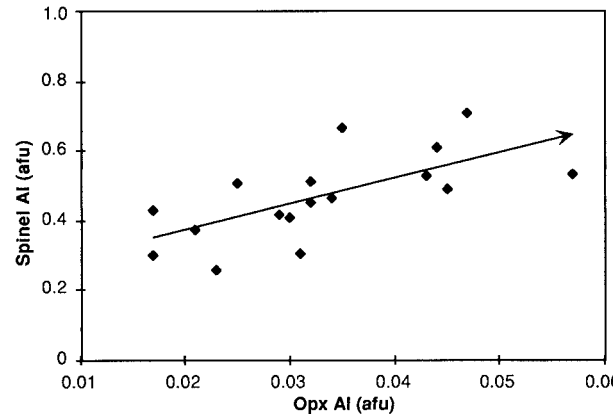

FIGURE 5. Concentrations of Al in chromite vs. Al in orthopyroxene for the 19 diogenites. Linear regression line shows a weak positive correlation, and arrow shows direction of crystallization trend. Outliers Ellemeet and ALHA 77256 have been removed. Afpu = atoms per formula unit.

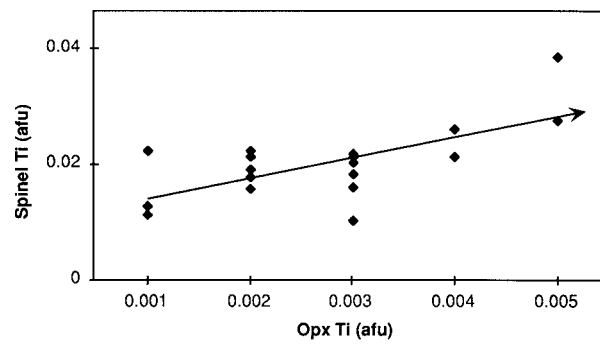

FIGURE 6. Concentrations of Ti in chromite vs. Ti in orthopyroxene. Linear regression line shows a weak positive correlation, and arrow shows direction of crystallization trend. Ellemeet has been removed because its Ti concentration is below the detection limits in orthopyroxene. Afpu = atoms per formula unit.

Chromite vs. orthopyroxene

In Figures 5 and 6, average Ti and Al for the analyzed chromite grains were plotted against average values for orthopyroxene reported by Fowler et al. (1994). These data reveal weak but apparent correlations between Al and Ti; similar trends are observed from LAP 91900 (0.26 apfu Al spinel, 0.02 apfu Al orthopyroxene) to LEW 88008 (0.71 apfu Al spinel, 0.05 apfu Al orthopyroxene), as noted above, with scatter from samples such as Ellemeet, Peckelsheim, EET 83246, and Manegaon.

DISCUSSION

The distribution of the major elements Fe and Mg in orthopyroxene from diogenites appears to have been modified by subsolidus reequilibration (Fowler et al. 1994; Mittlefehldt 1994), and it is obvious that the igneous signatures of Fe^{2+} and Mg in the chromites have been changed as well, given the relatively rapid diffusion rates of these two elements. However, the R^{3+} and R^{4+} cations, Cr, Al, and Ti, may have slow-enough diffusion rates to preserve a record of their igneous history (Roeder and Campbell 1985), and so were examined for zoning and core igneous signatures as well. If igneous signatures are preserved in the chromite grains, correlations between the compositions of igneous orthopyroxene and chromite grains should be evident.

The almost complete lack of zoning in the chromite grains is the first indication that the chromite grains apparently equilibrated with the surrounding orthopyroxenes (Sack et al. 1991; Mittlefehldt 1994; Bowman 1998). Even in cases where there is minimal zoning, the zoning is not typical of igneous fractionation, where compositional plateaus in the cores of the grains with increasing or decreasing concentrations at the rims would be expected. However, bulk magmatic compositional differences among the different samples are clearly identifiable. This is evident in virtually all the plots. Progressive differences in composition, indicating a magmatic relationship among the diogenites, are also evident.

Although these samples contain low concentrations of Ti, the variation in Ti appears to be systematic. The majority of the samples define a positive trend on the Ti vs. Al plot (Fig. 4). The substitutional coupling occurs from normal chromite structure to inverse ülvospinel, with Fe^{2+} and Ti^{4+} replacing Cr^{3+} or Al^{3+}. Within a normal crystallization sequence, chromite occurs as an earlier phase and ülvospinel as a later phase (Arai et al. 1996).

The most obvious trend that occurs in all the plots, based on a simple model of igneous fractionation, is from LAP 91900 crystallizing from the most primitive melt with low Al and Ti, and high Cr, to LEW 88008 being derived from the most evolved melt with high Al and Ti, and low Cr (Fig. 3). Consistent with the findings of Fowler et al. (1994), ALHA 77256, Roda and Ellemeet fall off virtually all trends. This is a potential indication of more than one magmatic source for the diogenites (cf. Fowler et al. 1994, 1995).

In the comparison plots of Al and Ti in chromite vs. orthopyroxene (Figs. 5 and 6), the trends are weak but significant. Titanium appears to show the best correlation, and Al shows only a modest correlation. This would be expected if Ti is least susceptible to diffusion or a better fractionation indicator. The spinel trend is the same trend observed for orthopyroxene between LAP 91900 as the most primitive and LEW 88008 as the most evolved, using a simple igneous fractionation sequence. This confirms the results of Fowler et al. (1994, 1995) found for orthopyroxenes.

IMPLICATIONS

The results of this study reveal an almost complete lack of zoning of the major and minor elements in chromite in this suite of samples, which indicates that the chromite grains have been able to equilibrate with the surrounding orthopyroxene. We infer that the Fe and Mg concentrations have been reset completely by subsolidus reequilibration. However, the Cr, Al, and Ti concentrations appear to retain some magmatic signature between samples. Based on a simple model of igneous fractionation, consistent compositional trends appear to be notable from LAP 91900 as the most primitive to LEW 88008, as the most evolved with high Al and Ti and low Cr. This trend can be seen in most of the plots and is similar to the results of the orthopyroxenes studied by Fowler et al. (1994). The outliers, ALHA 77256 and Roda, as well as Ellemeet, possibly indicate more than one magmatic source.

One of the most important observations in this work is the significant trend of decreasing Cr with increasing Al (Fig. 3) unlike that observed for spinel in lunar mare basalts. Similar results were reported by Mittlefehldt (1994). This systematic distribution is disrupted in mare basalts when plagioclase crystallization commences; in contrast, plagioclase does not crystallize during the interval when spinel crystallizes in diogenite parental melts. This provides additional evidence that the diogenite parent magmas were very unusual in their extreme Al depletion. We note that spinel grains from individual diogenites show a considerable range of Al, Cr, and Ti within the grain populations. Although igneous zoning, reactions between minerals and trapped melt, and subsolidus exchange contribute to the compositional variability, it is likely that in several meteorites mixing during brecciation also added to the compositional variability.

ACKNOWLEDGMENTS

This research was supported by NASA grant MRA 97-282 and the Institute of Meteoritics. Constructive reviews were provided by David Mittlefehldt and Alex Ruzicka as well as associate editor Brad Jolliff and editor Bob Dymek.

REFERENCES CITED

Arai, T., Takeda, H., and Warren, P.H. (1996) Four lunar mare meteorites: Crystallization trends of pyroxenes and spinels. Meteoritics & Planetary Science, 31, 877–892.

Bartels, K.S. and Grove, T.L. (1991) High-pressure experiments on magnesian eucrite compositions: Constraints on magmatic processes in the eucrite parent body. Proceedings of the 21st Lunar and Planetary Science Conference, 351–365.

Berkley, J.L. and Boynton, N.J. (1992) Minor/major element variation within and among diogenite and howardite orthopyroxenite groups. Meteoritics, 27, 387–394.

Binzel, R.P. and Xu, S. (1993) Chips off Asteroid 4 Vesta: Evidence for the parent body of basaltic achondrite meteorites. Science, 260, 186–191.

Bowman, L.E. (1998) Diogenites as asteroidal cumulates: Insights from automated EDS modal analysis and chromite chemistry. M.S. Thesis, Department of Earth and Planetary Sciences, University of New Mexico, 98 p.

Bowman, L.E., Spilde, M.N., and Papike, J.J. (1997) Automated EDS modal analysis applied to the diogenites. Meteoritics & Planetary Science, 32, 869–875.

Consolmagno, G.J. and Drake, M.J. (1977) Composition and evolution of the eucrite parent body: Evidence from rare earth elements. Geochimica et Cosmochimica Acta, 41, 1271–1282.

Drake, M.J. (1979) Geochemical evolution of the eucrite parent body: Possible nature and evolution of Asteroid 4 Vesta. In T. Gehrels, Ed., Asteroids, p. 765–782, University of Arizona Press.

Fowler, G.W., Papike, J.J., Spilde, M.N., and Shearer, C.K. (1994) Diogenites as asteroidal cumulates: Insights from orthopyroxene major and minor element chemistry. Geochimica et Cosmochimica Acta, 58, 3921–3929.

Fowler, G.W., Shearer, C.K., Papike, J.J., and Layne, G.D. (1995) Diogenites as asteroidal cumulates: Insights from orthopyroxene trace element chemistry. Geochimica et Cosmochimica Acta 59, 3071–3084.

Grove, T.L. and Bartels, K.S. (1992) The relation between diogenite cumulates and eucrite magmas. Proceedings of the 22nd Lunar and Planetary Science Conference, 437–445.

Mason, B. (1967) The Bununu meteorite, and a discussion of the pyroxene-plagioclase achondrites. Geochimica et Cosmochimica Acta, 31, 107–115.

Mittlefehldt, D.W. (1994) The genesis of diogenites and HED parent body petrogenesis. Geochimica et Cosmochimica Acta, 58, 1537–1552.

Papike, J.J., Hodges, F.N., Bence, A.E., Cameron, M., and Rhodes, J.M. (1976) Mare basalts: Crystal chemistry, mineralogy and petrology. Reviews of Geophysics and Space Physics, 14, 475–540.

Righter, K. and Drake, M.J. (1997) A magma ocean on Vesta: Core formation and petrogenesis of eucrites and diogenites. Meteoritics & Planetary Science, 32, 929–944.

Roeder, P.L. and Campbell, I.H. (1985) The effect of postcumulus reactions on composition of chrome-spinels from the Jimberlana Intrusion. Journal of Petrology, 26, 763–786.

Roeder, P.L. and Reynolds, I. (1991) Crystallization of chromite and chromium solubility in basaltic melts. Journal of Petrology, 32, 909–934.

Ruzicka, A., Snyder, G.A., and Taylor, L.A. (1997) Vesta as the howardite, eucrite, and diogenite parent body: Implications for the size of a core and for large-scale differentiation. Meteoritics & Planetary Science, 32, 825–840.

Sack, R.O., Azerado, W.J., and Lipschutz, M.E. (1991) Olivine diogenites: The mantle of the eucrite parent body. Geochimica et Cosmochimica Acta, 55, 1111–1120.

Shearer, C.K., Fowler, G. W., and Papike, J.J. (1997) Petrogenetic models for magmatism on the eucrite parent body: Evidence from orthopyroxene in diogenites. Meteoritics & Planetary Science, 32, 877–889.

Snetsinger, K.G, Bunch, T.E., and Keil, K. (1968) Electron microprobe analysis of vanadium in presence of titanium. American Mineralogist, 53, 1770–1773.

Stolper, E. (1977) Experimental petrology of eucrite meteorites. Geochimica et Cosmochimica Acta, 41, 587–611.

Takeda, H. (1997) Mineralogical records of early planetary processes on the howardite, eucrite, diogenite parent body with reference to Vesta. Meteoritics & Planetary Science, 32, 841–853.

Takeda, H., Miyamoto, M., Ishii, T., and Yanai, K. (1979) Mineralogical examination of the Yamato-75 Achondrites and their layered crust model. Proceedings of the 3rd Symposium on Antarctic Meteorites, 82–108.

Warren, P.H. (1985) Origin of howardites, diogenites, and eucrites: A mass balance constraint. Geochimica et Cosmochimica Acta, 49, 577–586.

——(1997) Magnesium oxide-iron oxide mass balance constraints and a more detailed model for the relationship between eucrites and diogenites. Meteoritics & Planetary Science, 32, 945–963.

Warren, P.H. and Jerde, E.A. (1987) Composition and origin of Nuevo Laredo trend eucrites. Geochimica et Cosmochimica Acta, 51, 713–725.

MANUSCRIPT RECEIVED JUNE 18, 1998
MANUSCRIPT ACCEPTED FEBRUARY 16,1999
PAPER HANDLED BY BRAD L. JOLLIFF